Roma International Conference on AstroParticle Physics

LHAASO Discovery of an Ultrahigh-energy gamma-ray Bubble in Cygnus X

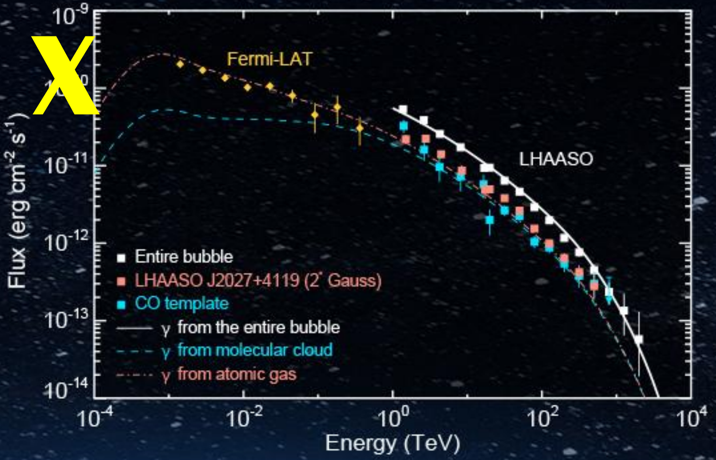

Ruo-Yu Liu (for LHAASO Collaboration)
School of Astronomy and Space Science,
Nanjing University

based on the publication
LHAASO Coll. 2024, *Science Bulletin*, 69, 449
arXiv:2310.10100

25.09.2024, RICAP 2024, Frascati, Italy

Outline

- A Brief Review of Previous Studies (observational & theoretical)
- Observation of Cygnus Bubble by LHAASO and Modelling
- Discussion & Summary

Origin of Cosmic Rays

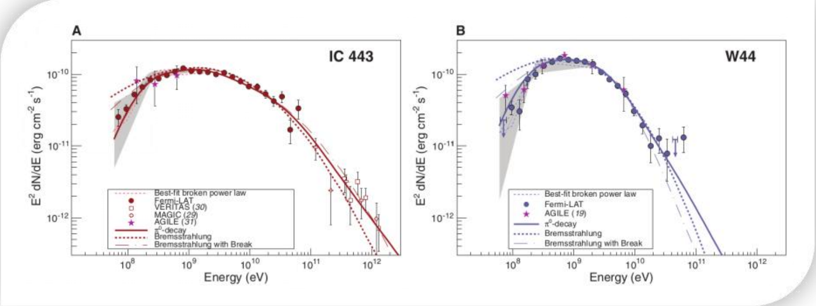

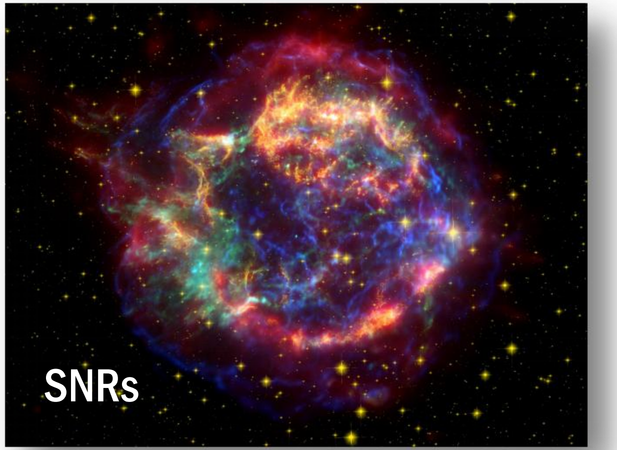

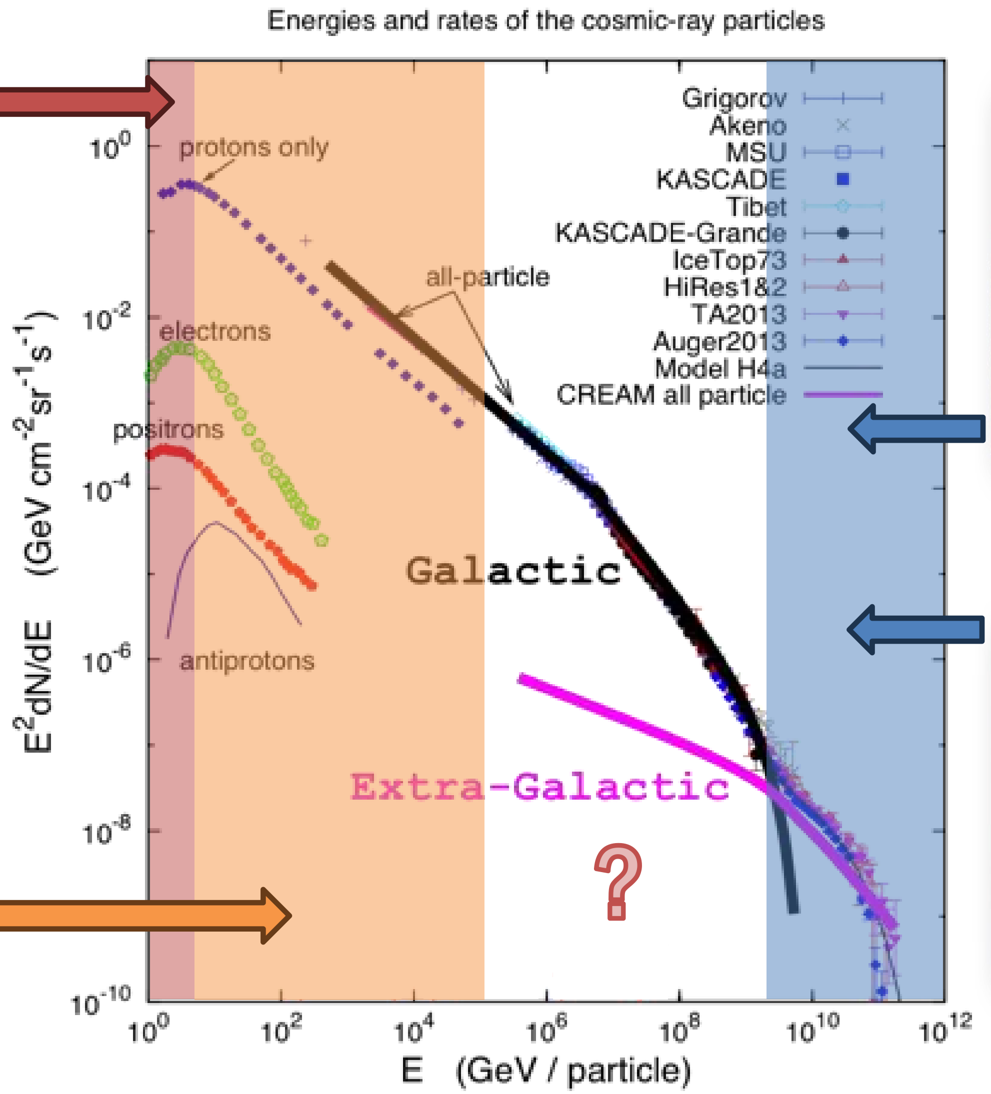

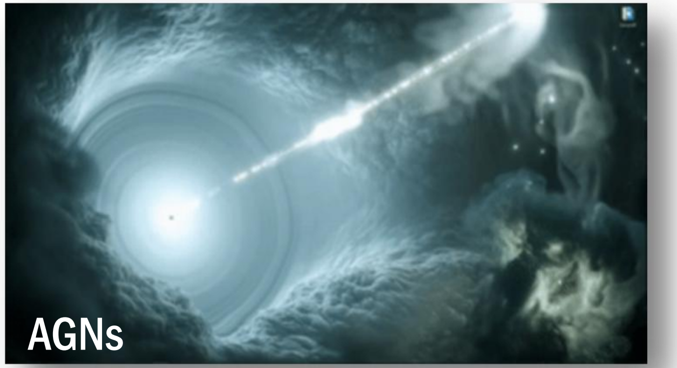

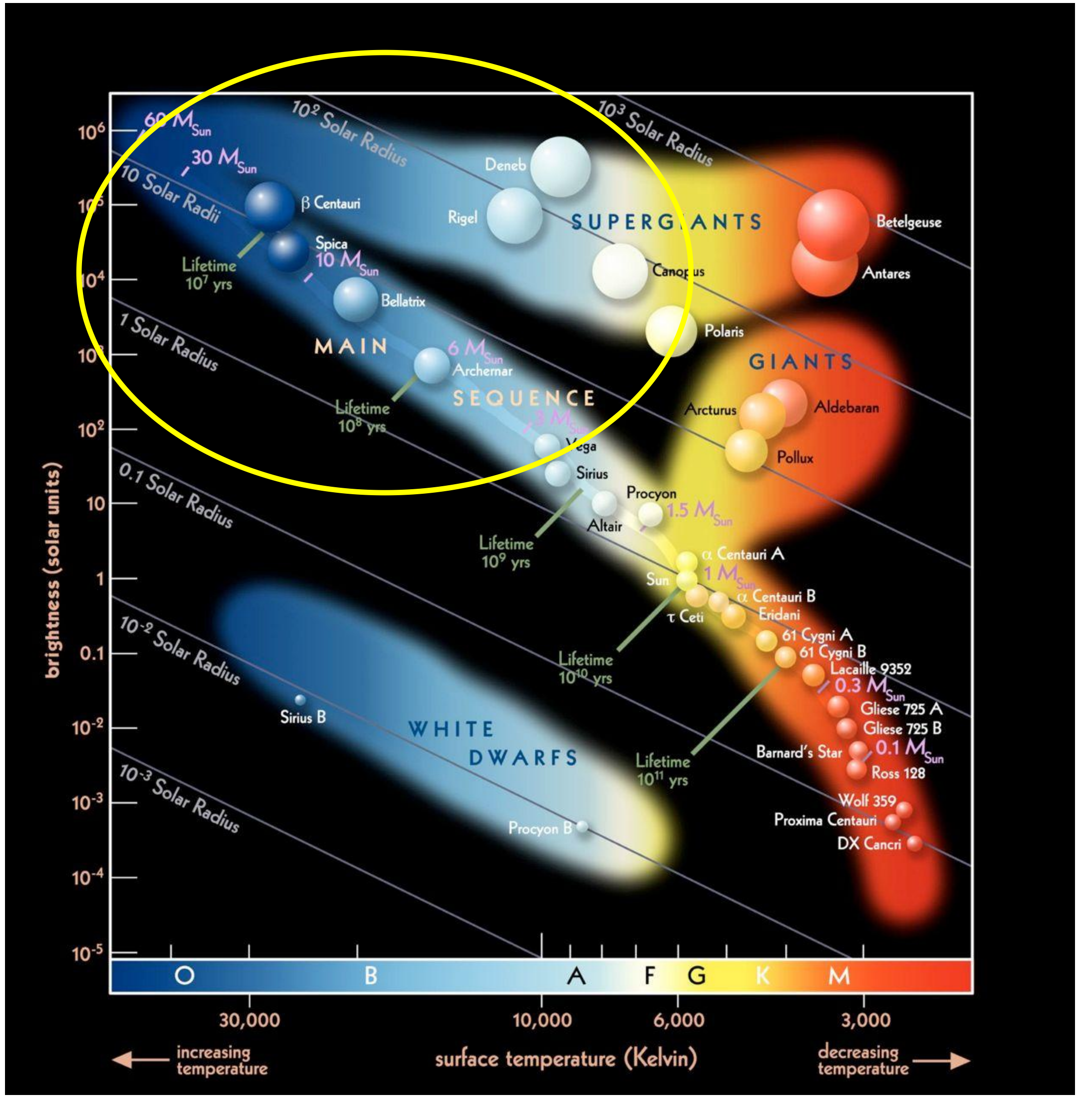

Massive stellar winds as CR accelerators

Casse & Paul 1980

TABLE 1

DISTANCES BETWEEN THE SHOCK AND THE STAR FOR DIFFERENT KINDS OF STARS IN DIFFERENT ENVIRONMENTS

Distance between the shock and the star (pc)	18	5.2	5.7	1.6
Star:				
Mass loss rate ($M_\odot$ yr^{-1})	10^{-5}	10^{-5}	10^{-6}	10^{-6}
Wind velocity (km s^{-1})	2000	2000	2000	2000
Surrounding medium:				
Density n (particles cm^{-3})	1	10^3	1	10^3
Temperature[a] (K)	10^4	20	10^5	20
Magnetic field strength (μG)	3	30	3	30
Cosmic ray energy density (eV cm^{-3})	1	1	1	1
Pressure (10^{-12} dynes cm^{-2}):				
Due to gas: p_G	2.8	2.8	2.8	2.8
Due to magnetic field: p_B	0.36	36	0.36	36
Due to cosmic rays: p_{CR}	0.15	0.15	0.15	0.15
Total due to ISM: p_i	3.3	39	3.3	39

Provided the acceleration is not intermittent, and in the optimum case, the highest energies that cosmic rays of charge Z can attain at stellar wind terminal shock are:

$$E_{\max} = 4 \times 10^6\, Z(B/10^{-5}\,\mathrm{G})\,(w/2.5 \times 10^8\,\mathrm{cm\,s^{-1}})^2\ \mathrm{GeV}$$

whereas for supernova shocks, under similar conditions:

$$E_{\max} < 10^5\, Z(B/10^{-6}\,\mathrm{G})\ \mathrm{GeV}\,,$$

Cesarsky & Montemerle 1983

Gamma-ray as Probes of Hadronic CR Accelerators

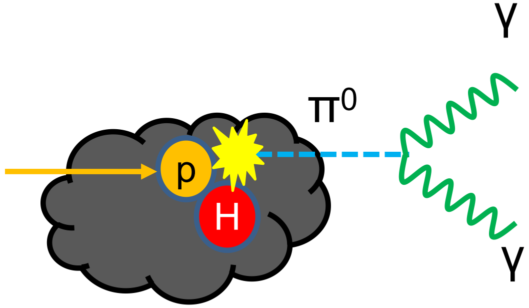

CR Spatial distribution

$u_{cr} \sim L/r$ continous injection+Diffusion

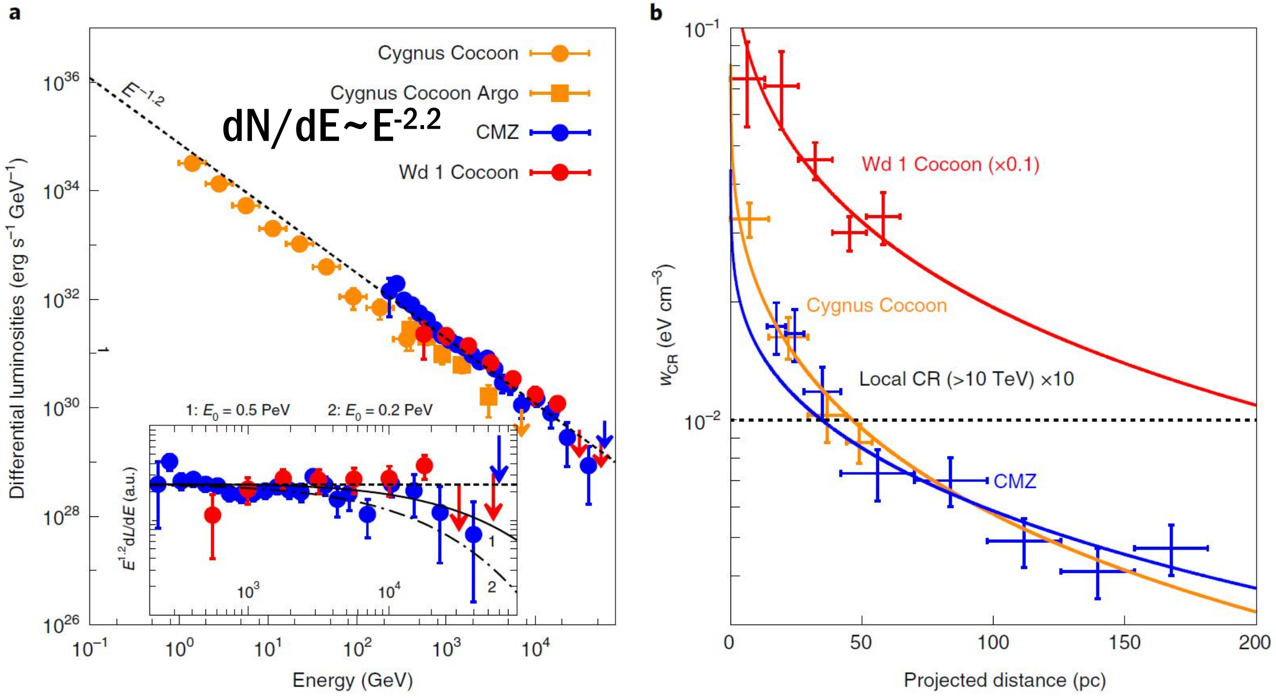

Table 1 | Physical parameters of three extended γ-ray structures and their related stellar clusters

Source	Cygnus Cocoon	CMZ	Wd 1 Cocoon
Extension (pc)	50	175	60
Age of cluster (Myr)[39]	3–6	2–7	4–6
Kinetic luminosity, L_{kin}, of cluster (erg s^{-1})	2×10^{38} (ref. [17])	1×10^{39} (ref. [40])	1×10^{39} (ref. [41])
Distance (kpc)	1.4	8.5	4
ω_0 (>10 TeV) (eV cm^{-3})	0.05	0.07	1.2

Aharonian et al. 2019

Particle acceleration in star clusters

Colliding shocks

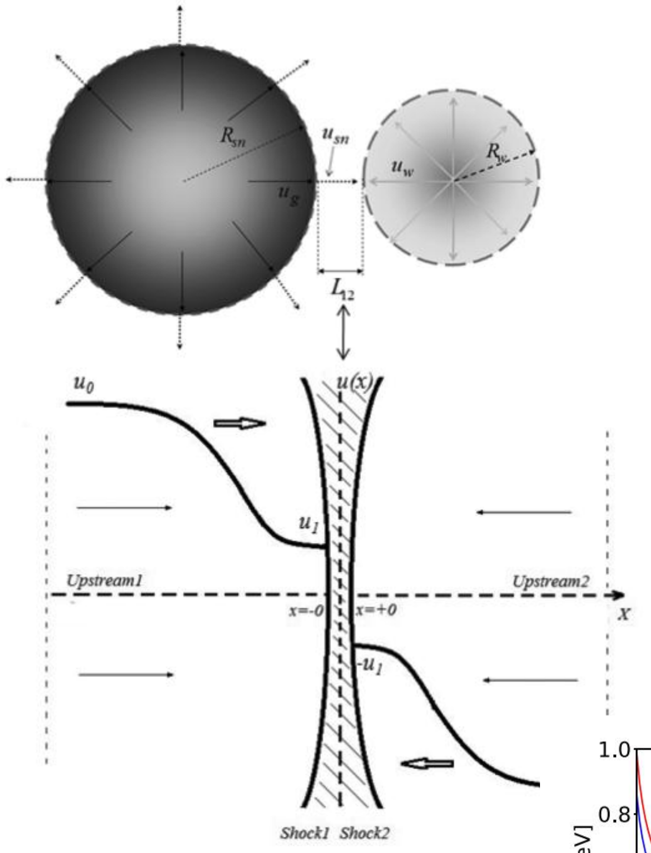

Bykov et al. 2013

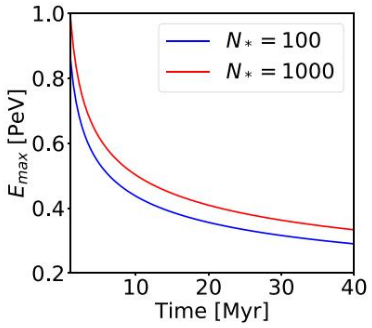

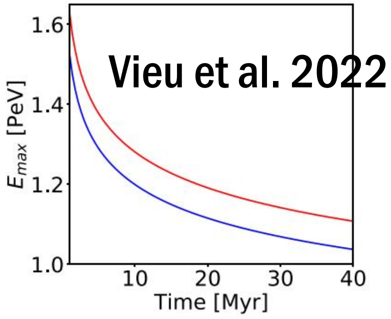

Vieu et al. 2022

Collective wind termination shocks

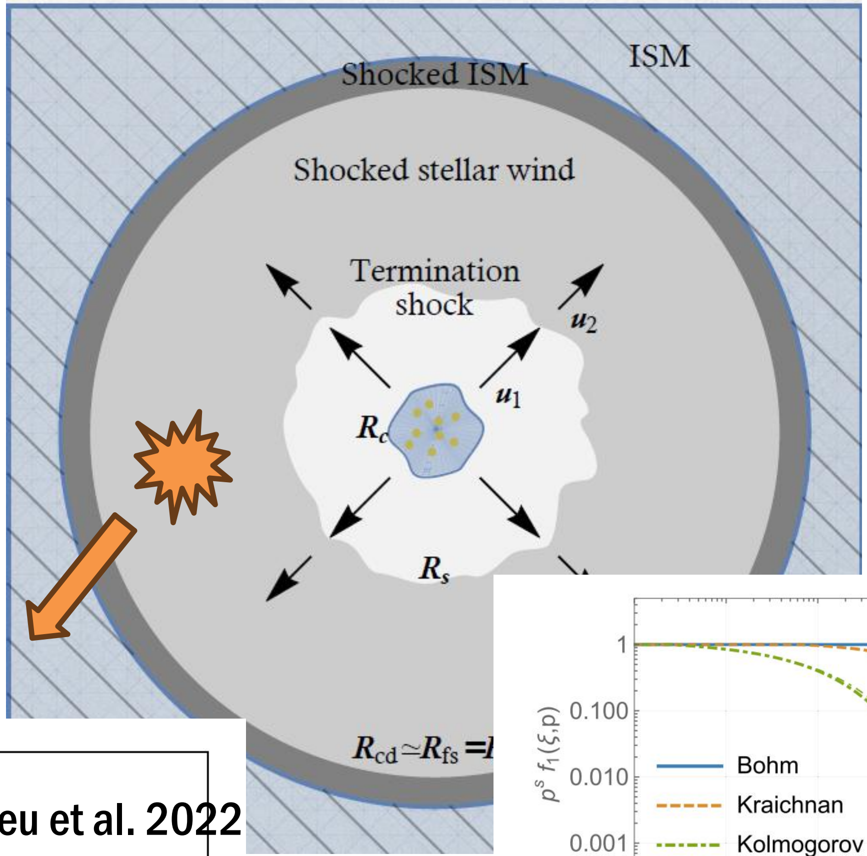

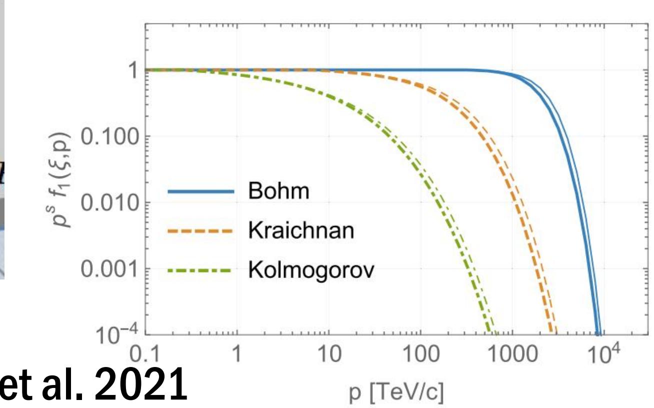

Morlino et al. 2021

Previous Gamma-ray Observation of Cygnus Star-forming region

Cygnus X: an intense star-forming region close to Earth (1.4-1.7 kpc)

extension ~ 200 pc

hundreds of O stars, thousands of B stars

several $\mathrm{x}10^6\ M_\odot$ solar mass in gas

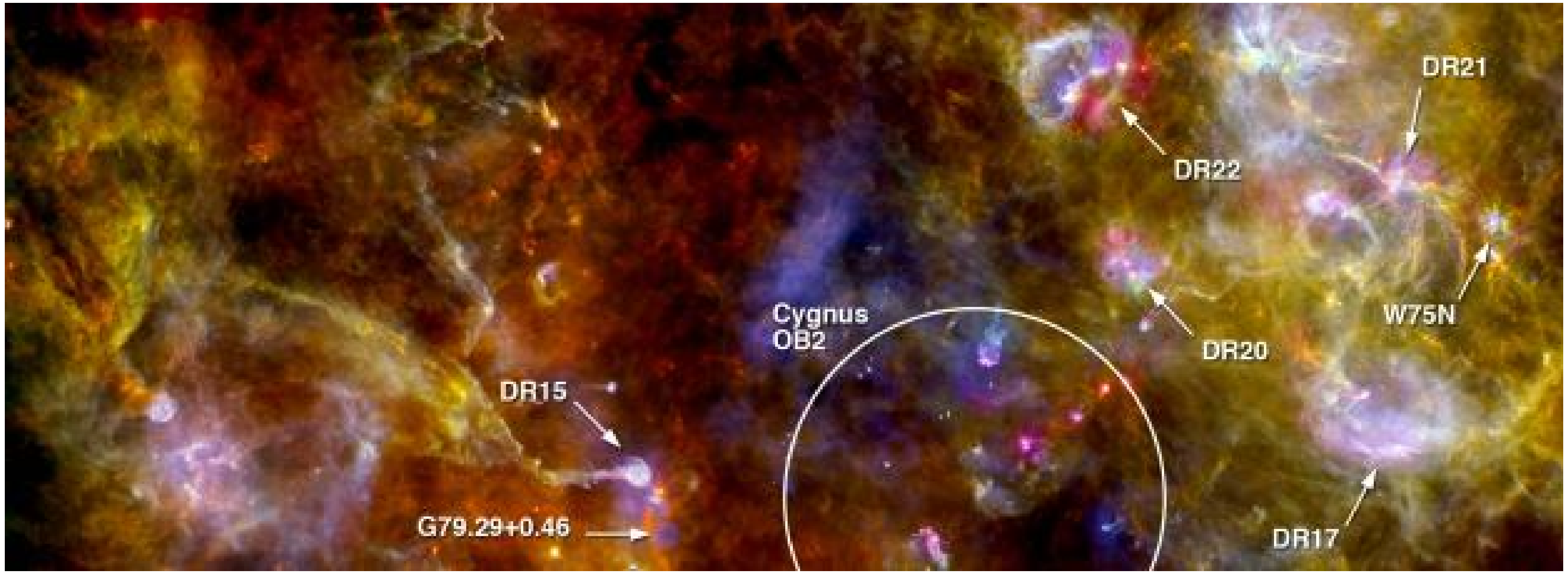

Credit： ESA/Herschel Space Observatory

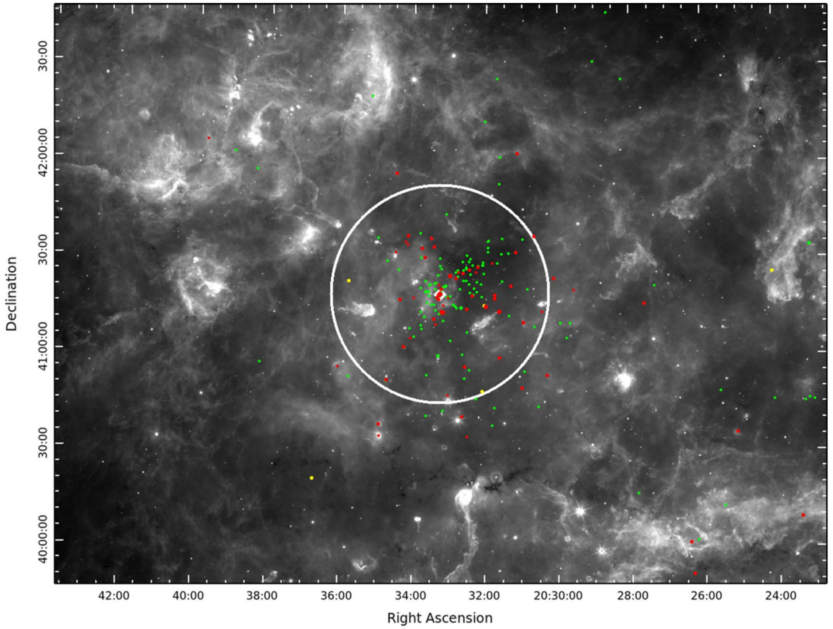

Wright et al. 2015

Fermi-LAT Collaboration 2011

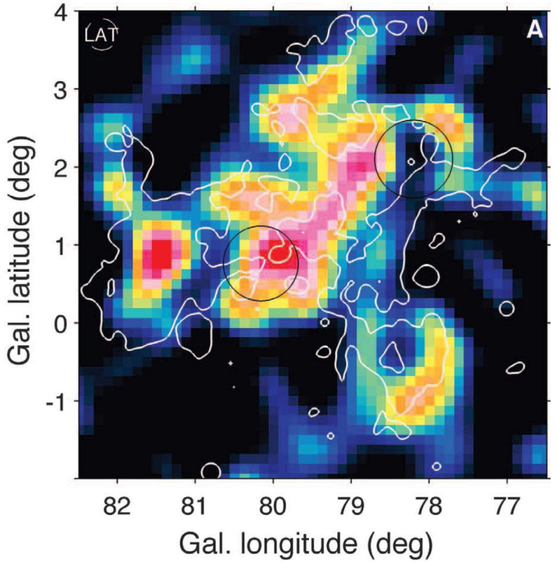

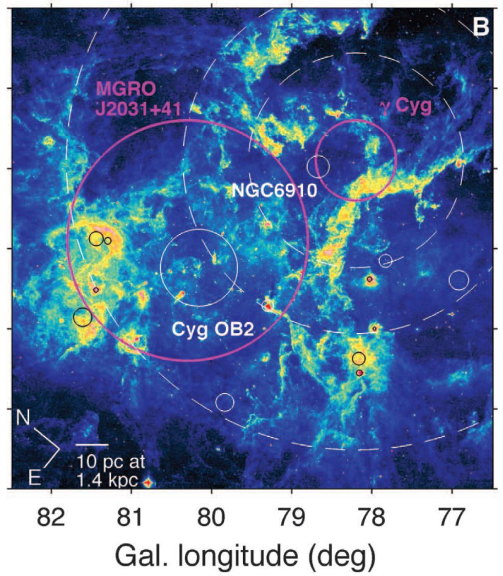

Abeysekara et al., Nature Astronomy (2021)

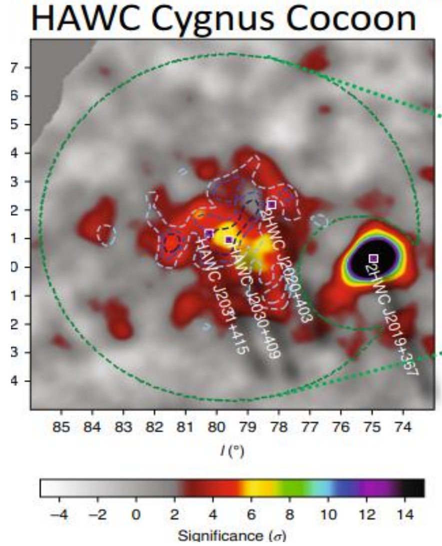

Galactic Coordinates

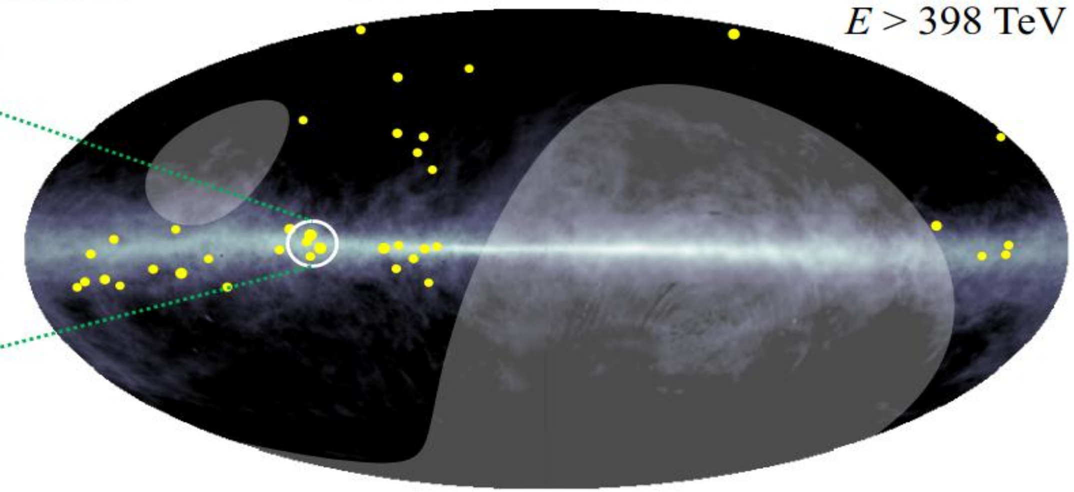

Asgamma Collaboration 2021

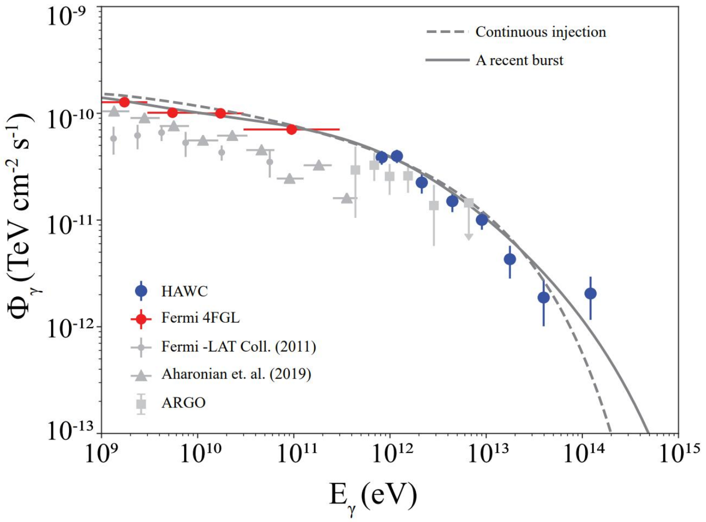

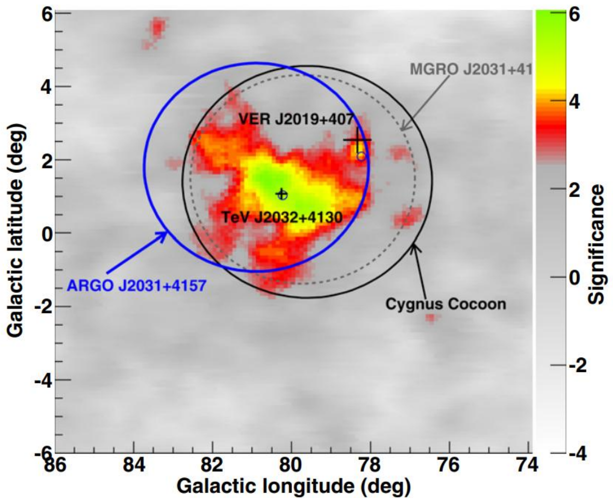

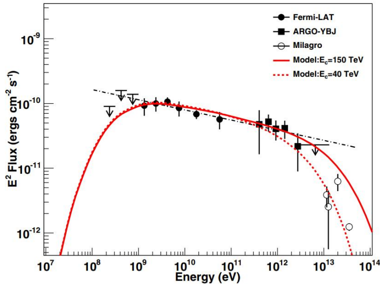

ARGO Collaboration 2014

LHAASO's Observation

Source name	RA (°)	dec. (°)	Significance above 100 TeV (×σ)	E_{max} (PeV)	
LHAASO J0534+2202	83.55	22.05	17.8	0.88 ± 0.11	
LHAASO J1825-1326	276.45	−13.45	16.4	0.42 ± 0.16	
LHAASO J1839-0545	279.95	−5.75	7.7	0.21 ± 0.05	
LHAASO J1843-0338	280.75	−3.65	8.5	$0.26_{-0.10}^{+0.16}$	
LHAASO J1849-0003	282.35	−0.05	10.4	0.35 ± 0.07	
LHAASO J1908+0621	287.05	6.35	17.2	0.44 ± 0.05	
LHAASO J1929+1745	292.25	17.75	7.4	$0.71_{-0.07}^{+0.16}$	
LHAASO J1956+2845	299.05	28.75	7.4	0.42 ± 0.03	0.41(0.09)
LHAASO J2018+3651	304.75	36.85	10.4	0.27 ± 0.02	0.50(0.10)
LHAASO J2032+4102	308.05	41.05	10.5	1.42 ± 0.13	0.54(0.10)
LHAASO J2108+5157	317.15	51.95	8.3	0.43 ± 0.05	0.38(0.09)
LHAASO J2226+6057	336.75	60.95	13.6	0.57 ± 0.19	1.05(0.16)

Celestial coordinates (RA, dec.); statistical significance of detection above 100 TeV (calculated using a point-like template for the Crab Nebula and LHAASO J2108+5157 and 0.3° extension templates for the other sources); the corresponding differential photon fluxes at 100 TeV; and detected highest photon energies. Errors are estimated as the boundary values of the area that contains ±34.14% of events with respect to the most probable value of the event distribution. In most cases, the distribution is a Gaussian and the error is 1σ.

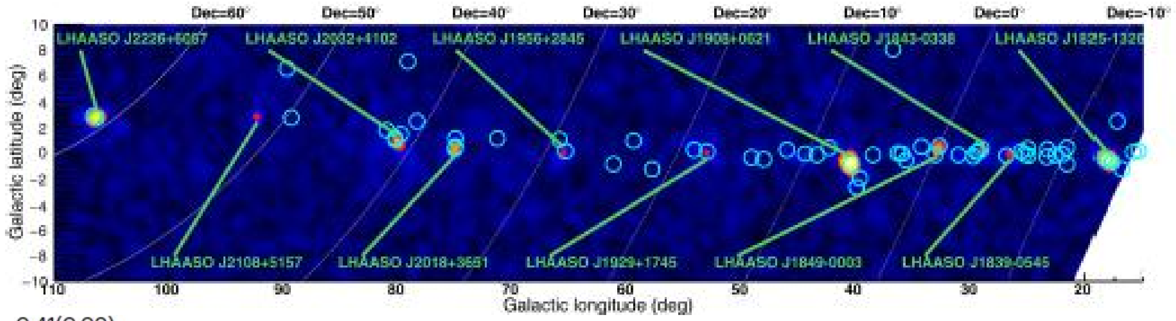

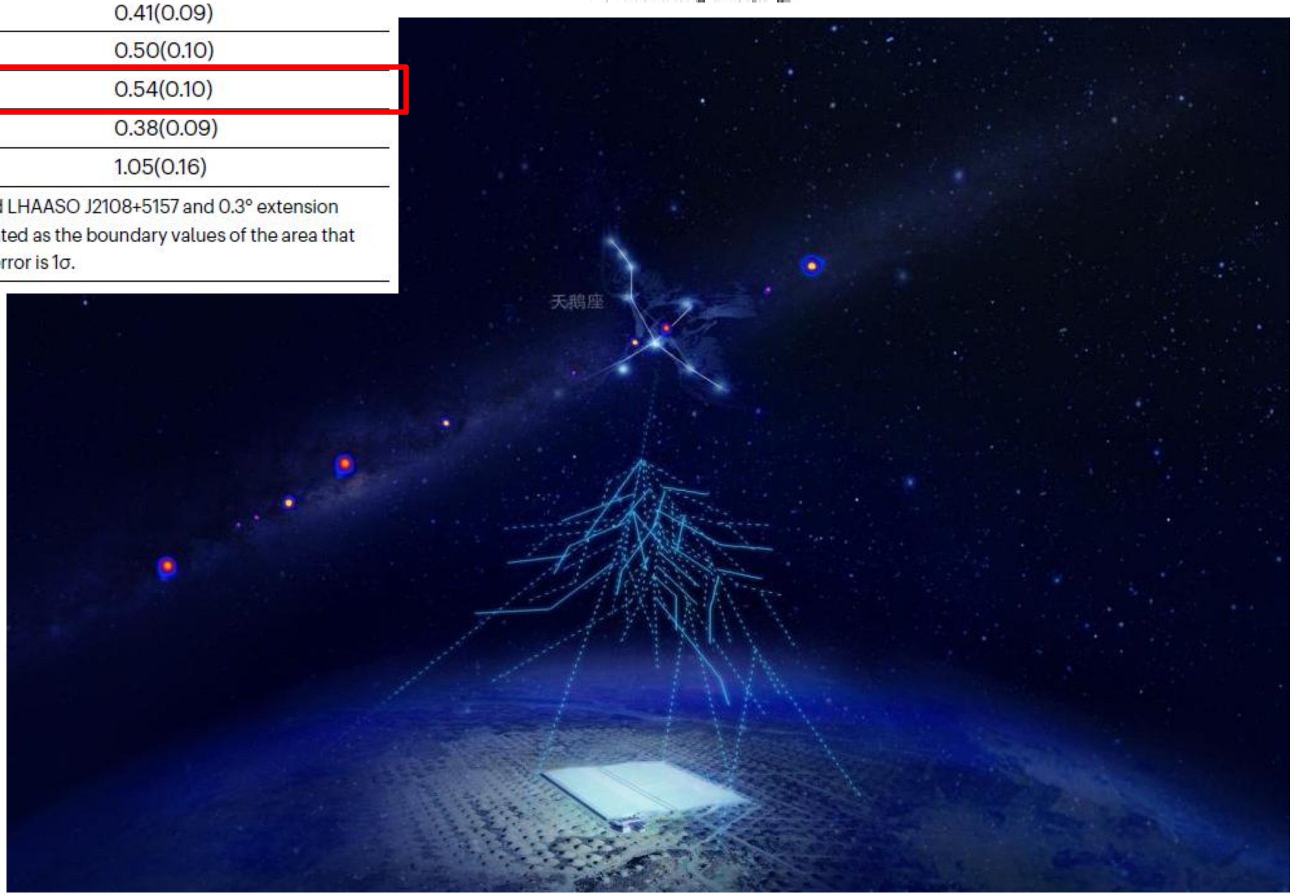

0.54 Crab flux @ 100TeV within 0.3deg of the best-fit position

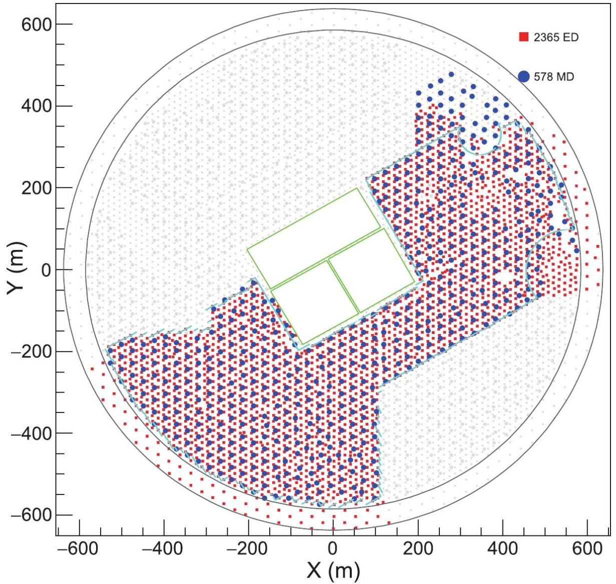

Half array over 11 months

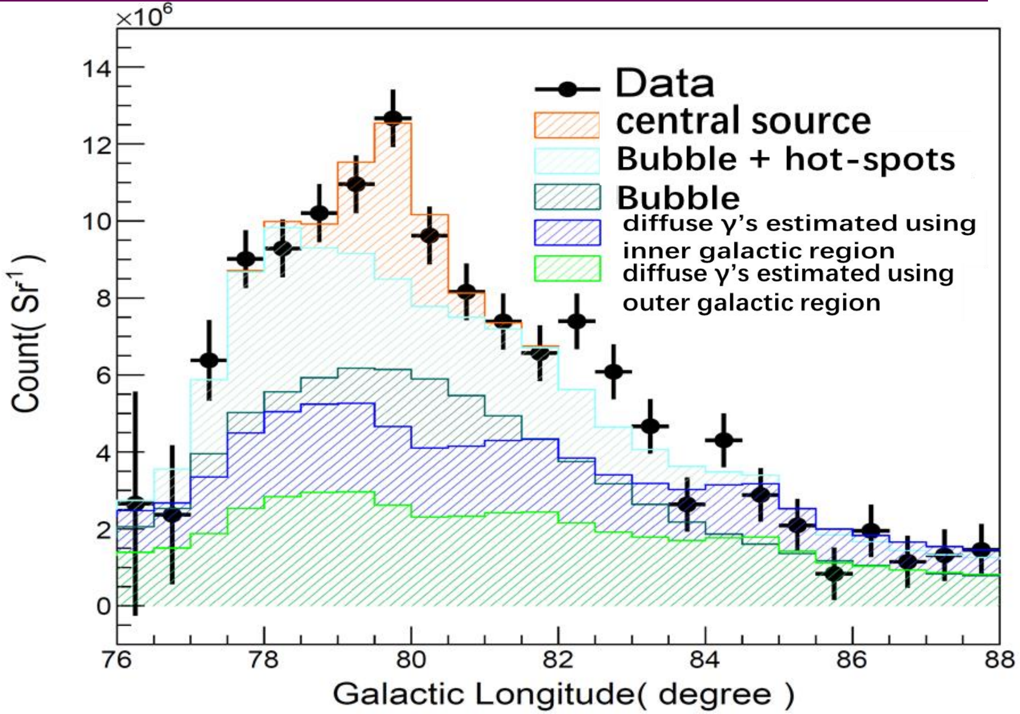

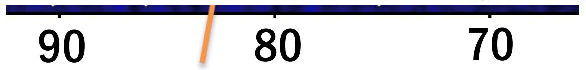

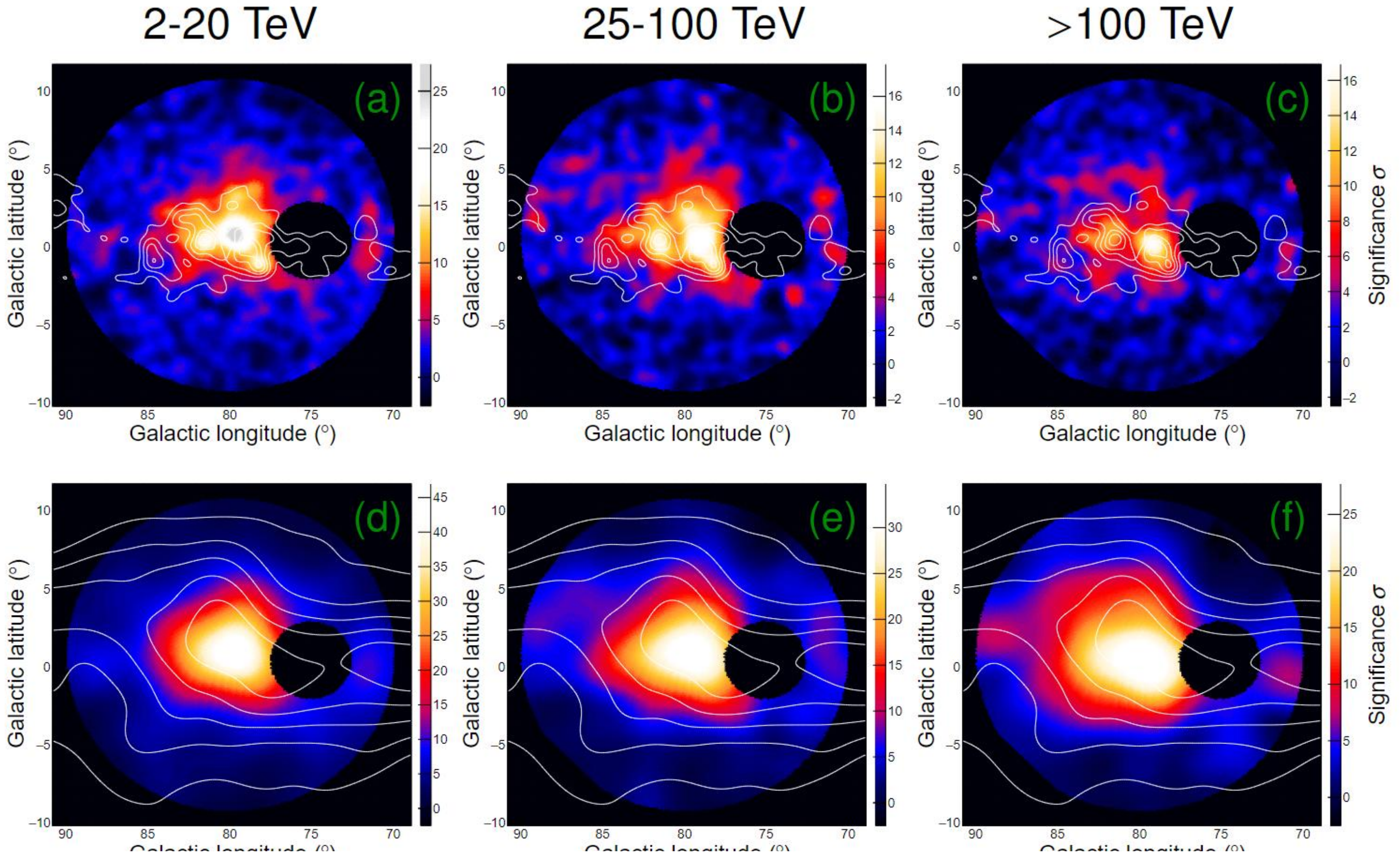

Source	Components	$\alpha_{2000}(\circ)$	$\delta_{2000}(\circ)$	$r_{39}(\circ)$	TS	$N_0(TeV^{-1}m^{-2}s^{-1})$	Γ
LHAASO J2027+4119	KM2A	307.43 ± 0.16	41.05 ± 0.13	2.17 ± 0.10	145	$(0.62 \pm 0.05) \times 10^{-15}$@$50TeV$	-2.99 ± 0.07
	WCDA	306.90 ± 0.23	41.33 ± 0.16	2.28 ± 0.14	251.44	$(1.27 \pm 0.14) \times 10^{-9}$@$7TeV$	-2.63 ± 0.08
HI	KM2A				108	$(0.69 \pm 0.10) \times 10^{-15}$@$50TeV$	-2.94 ± 0.12
	WCDA				60.77	$(1.43 \pm 0.26) \times 10^{-9}$@$7TeV$	-2.66 ± 0.12
MC	KM2A				88	$(0.46 \pm 0.06) \times 10^{-15}$@$50TeV$	-2.87 ± 0.14
	WCDA				67.47	$(1.08 \pm 0.19) \times 10^{-9}$@$7TeV$	-2.73 ± 0.13
LHAASO J2031+4057	WCDA	307.89 ± 0.09	40.96 ± 0.16	0.33 ± 0.08	115.40	$(0.11 \pm 0.06) \times 10^{-9}$@$7TeV$	-2.75 ± 0.17

Concentration of UHE photons

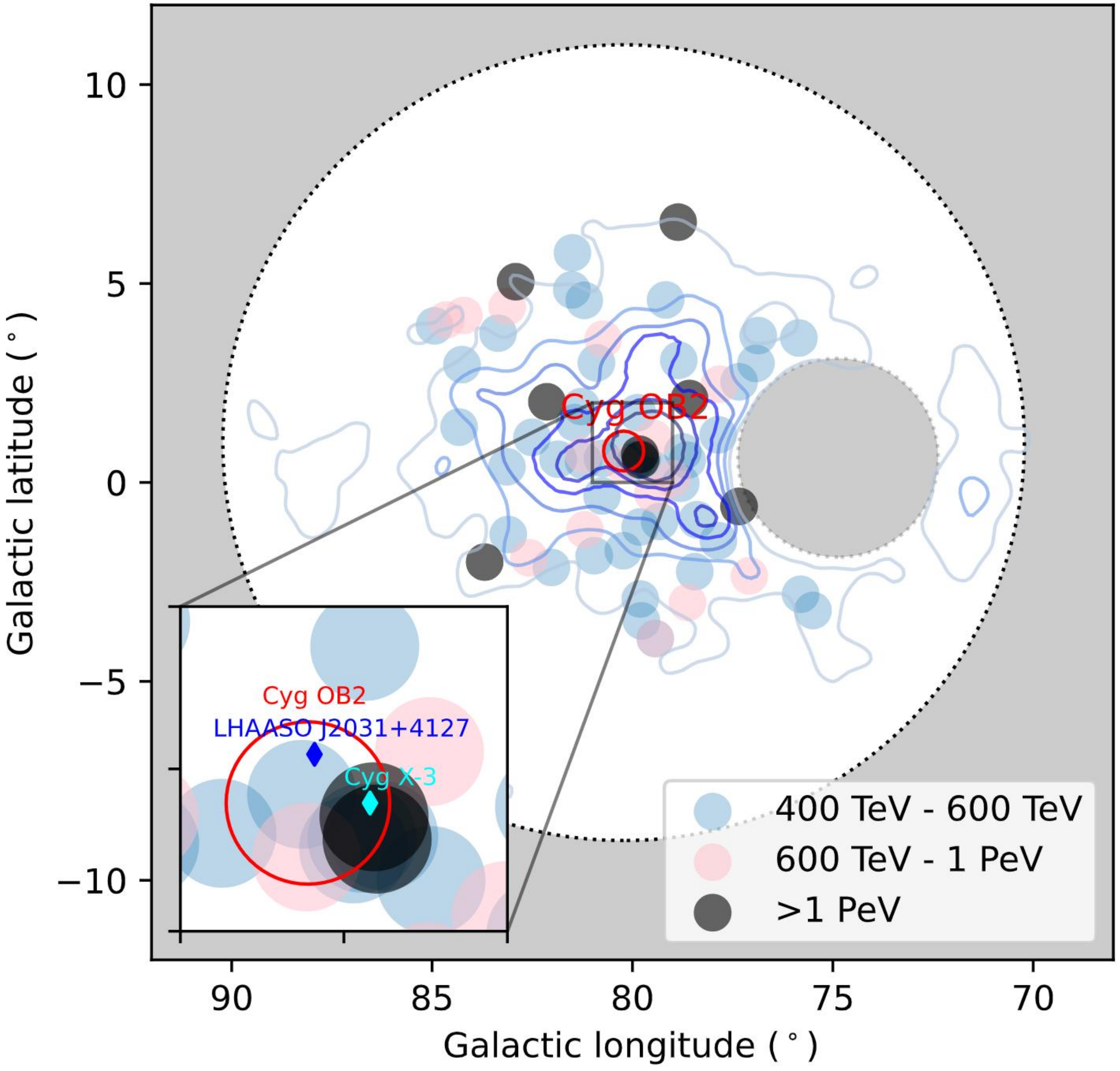

66 photon-like events within a radius of 6 degree with an estimated background of 9.5

8 photons above 1 PeV

E (PeV)	δE (PeV)	N_e	N_μ	$\theta(^\circ)$	$D_{edge}(m)$	$\psi(^\circ)$
1.08	0.16	5904	13.0	19.4	143	4.7
1.19	0.18	5480	14.1	34.4	73	0.2
1.20	0.18	6939	12.6	14.2	132	5.8
1.35	0.20	6938	8.4	27.1	43	2.9
1.38	0.20	6469	8.9	17.4	52	2.6
1.42	0.21	6258	6.6	12.7	57	0.1
1.78	0.27	6665	12.8	18.0	41	1.8
2.48	0.37	13815	29.1	33.0	99	5.2

7/66 from central 0.5 deg region v.s. $66*(0.5/6)^2 \approx 0.5$

2/8 PeV event from central 0.5 deg region

Overdensity at the centre – injection!

Spectral Energy Distribution of the Bubble

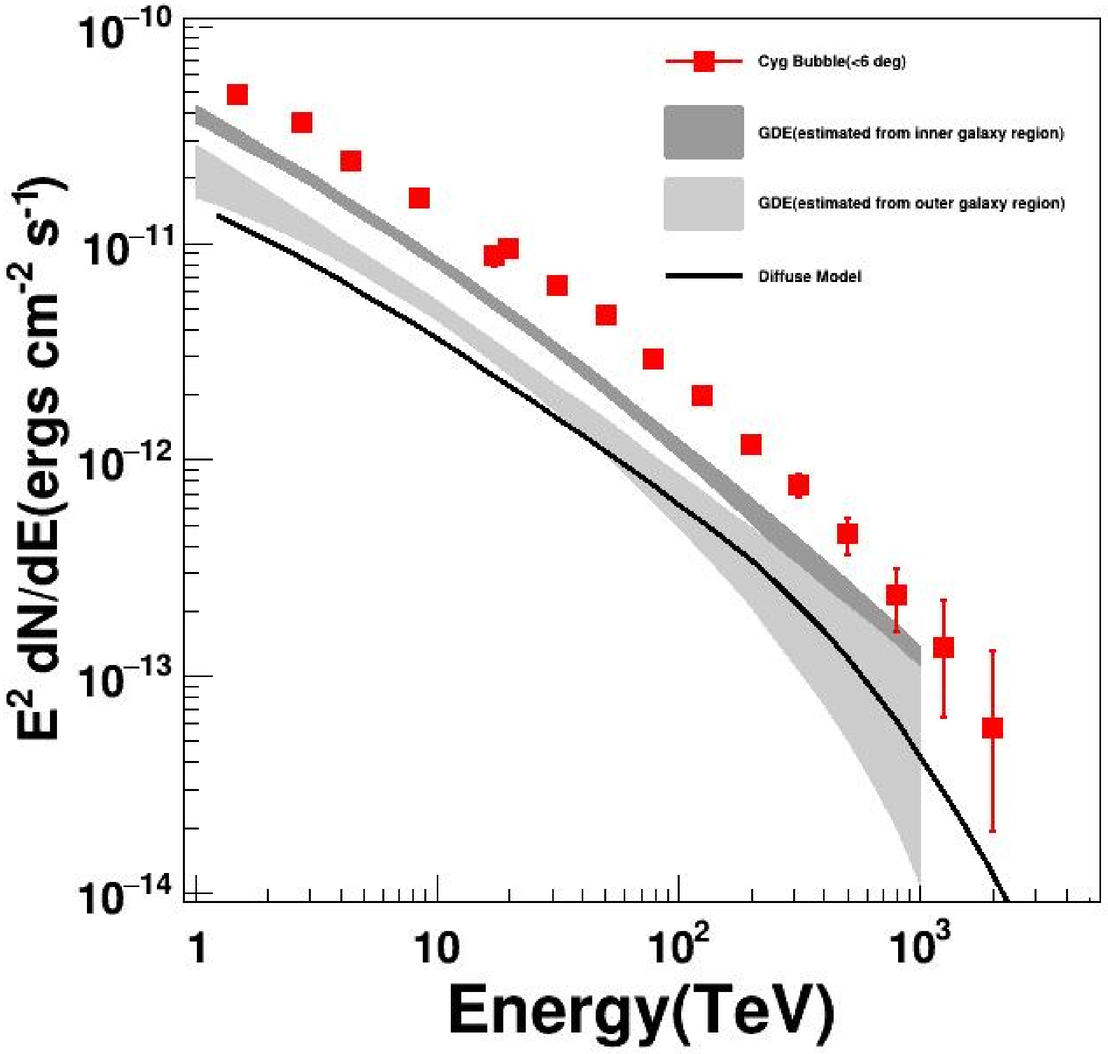

Energy Bin	Non	Nb
400TeV-630TeV	42	6.8
630TeV-1PeV	14	1.9
1PeV-1.6PeV	6	0.6
1.6PeV-2.5PeV	2	0.2

Almost background free

- ◆The spectrum spans 3 decades up to 2 PeV
- ◆Spectral index ~ 2.7
- ◆No indication of cut-off in the spectrum

Physical Picture

- High energy cosmic rays escape from the accelerator in the core region
- producing gamma rays via interactions with surrounding medium
- Slow diffusion ~1% of the standard ISM Diffusion coefficient

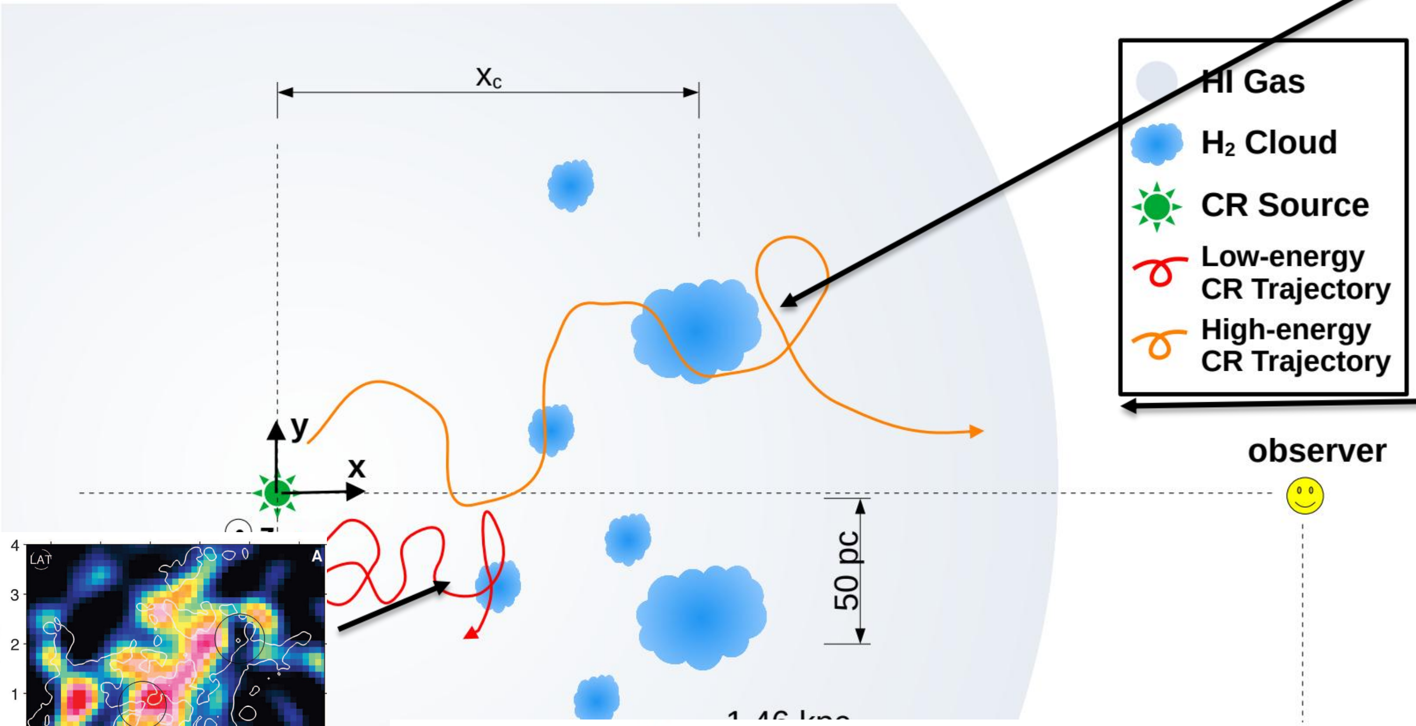

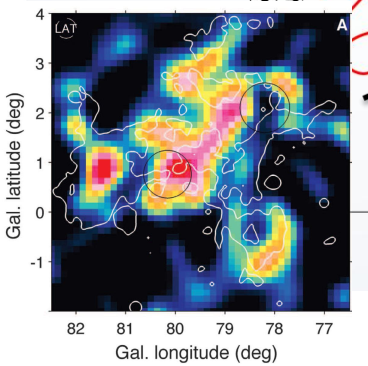

$$n_{\rm HI}(x,y,z) = \frac{M_{\rm HI}}{(2\pi)^{3/2}\sigma_{\rm HI}^3 m_{\rm H}} \exp\left\{-[x^2+y^2+z^2]/2\sigma_{\rm HI}^2\right\} + n_0$$

$$n_{\rm MC}(x,y,z) = \frac{M_{\rm MC}}{(2\pi)^{3/2}\sigma_{\rm MC}^3 m_{\rm H}} \exp\left\{-[x-x_{\rm MC})^2+(y-y_{\rm MC})^2+z^2]/2\sigma_{\rm MC}^2\right\} + n_1$$

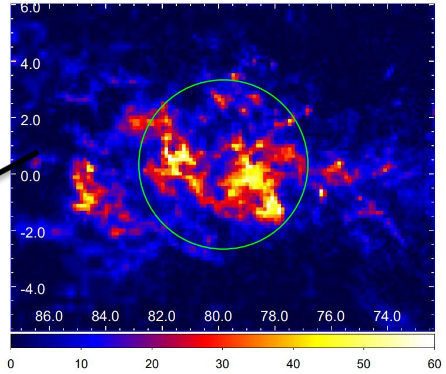

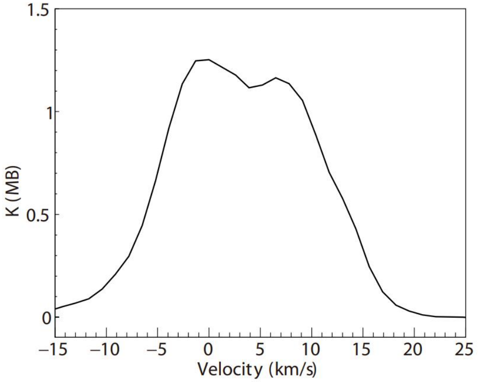

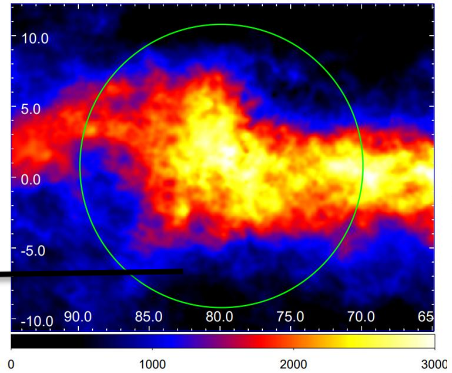

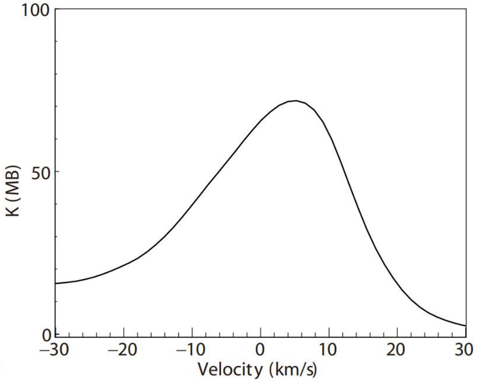

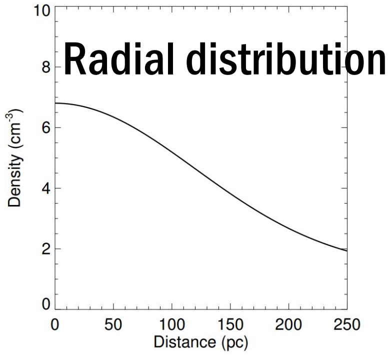

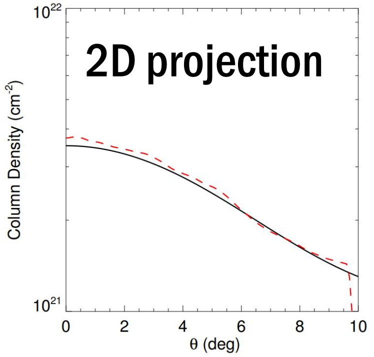

Modeling SED of different components

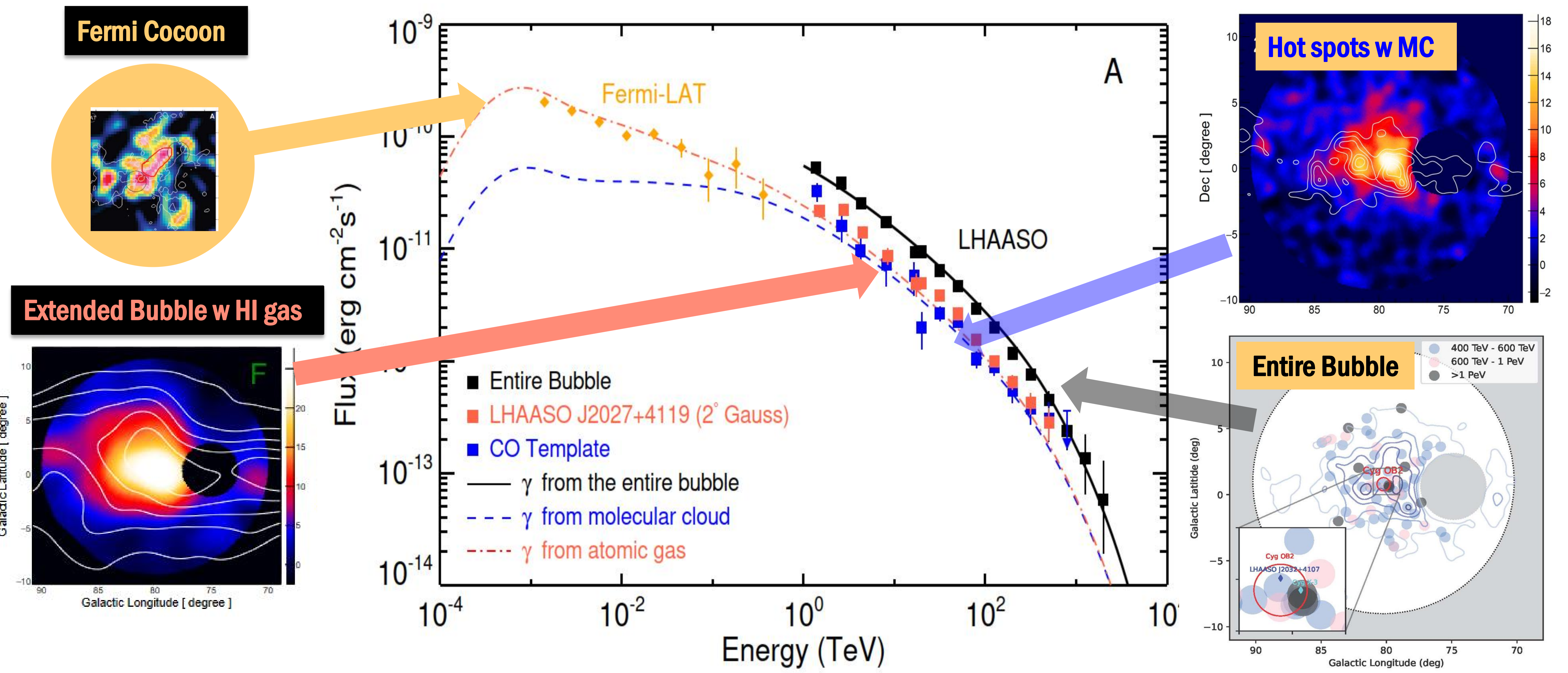

1D intensity profile

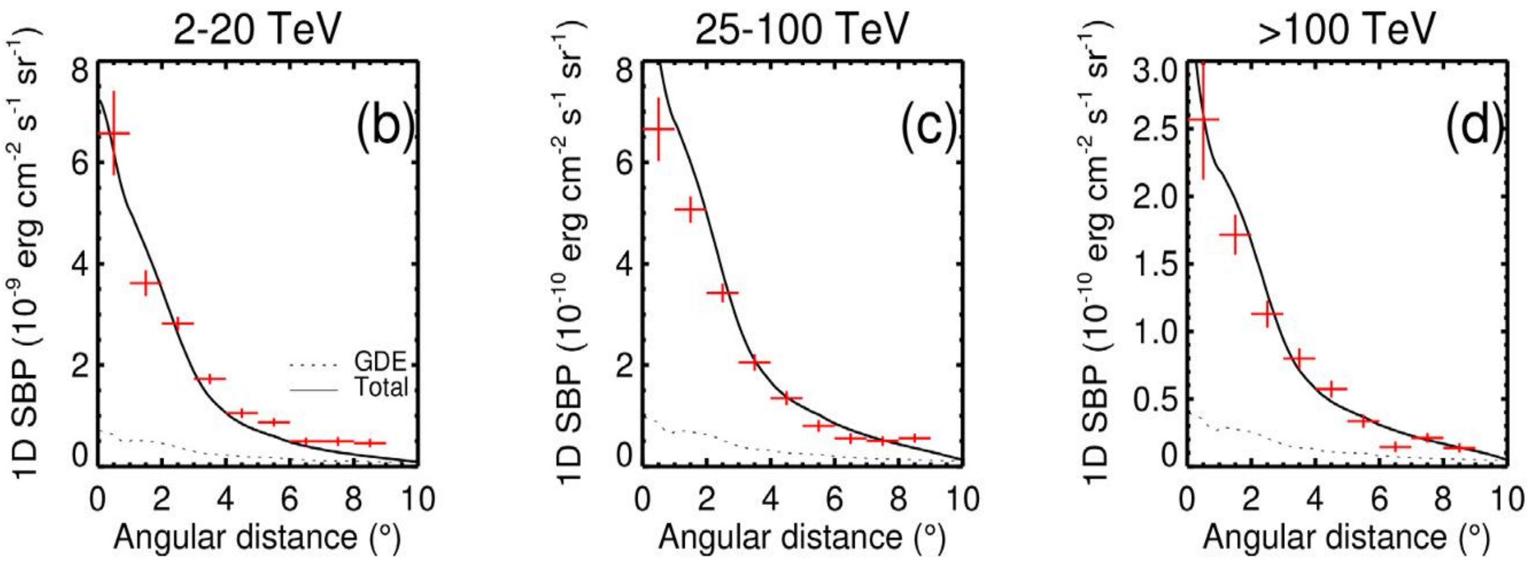

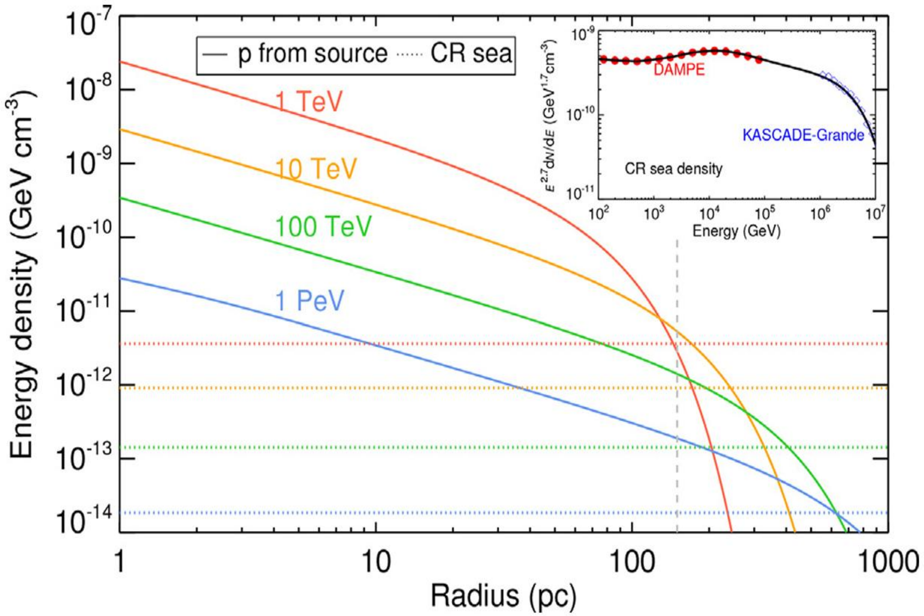

- 1D intensity profile can be explained simultaneously
- Profile is determined by both CR distribution and gas distribution
- No sharp boundary of the bubble, depending on the level of diffuse γ-rays

Constant injection rate →n(r) ~ 1/r
For impulsive injection →n(r) ~ const
Within $r < r_{diff}$

accurate 3D gas distribution is crucial!

Galactic mini starburst W43

- Galactic mini star burst. 5.5kpc from Earth
- Contribute 10% of the Galactic star formation rate
- Huge HII region excited by central WR/OB cluster
- GeV detection by Fermi-LAT

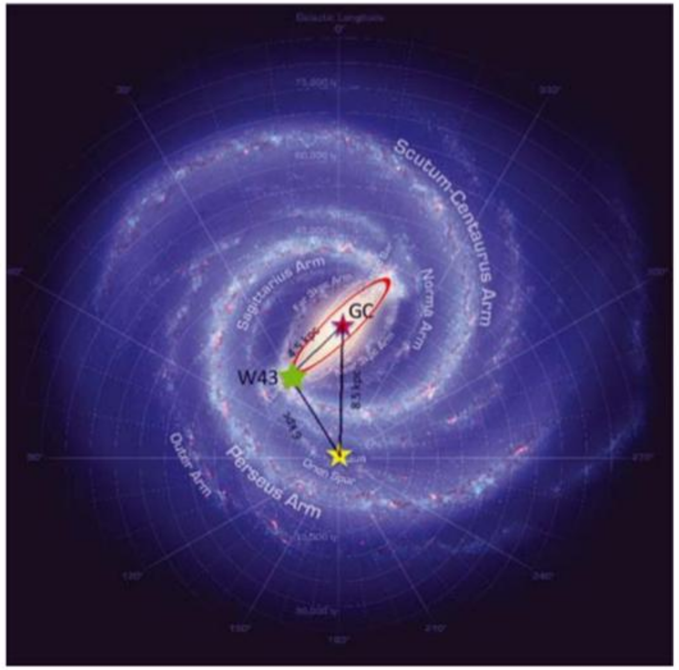

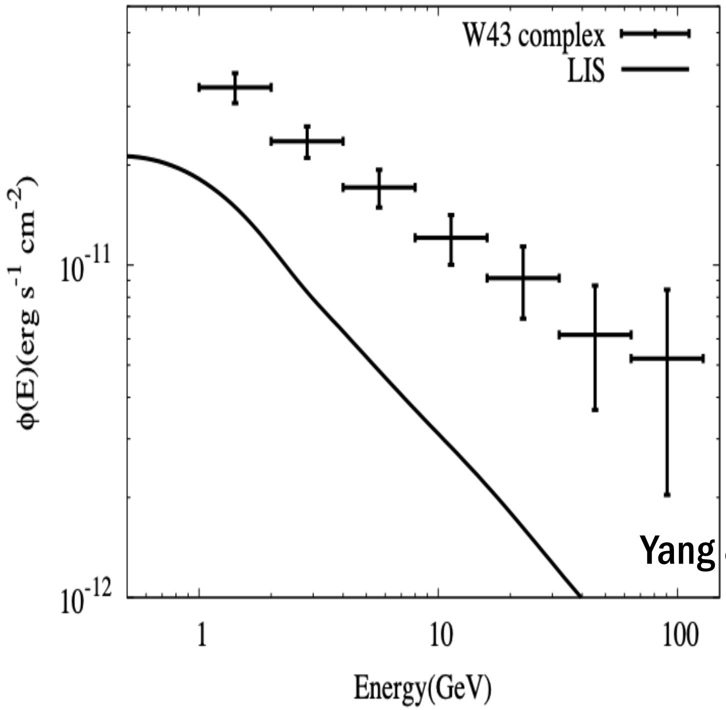

Yang & Wang 2020

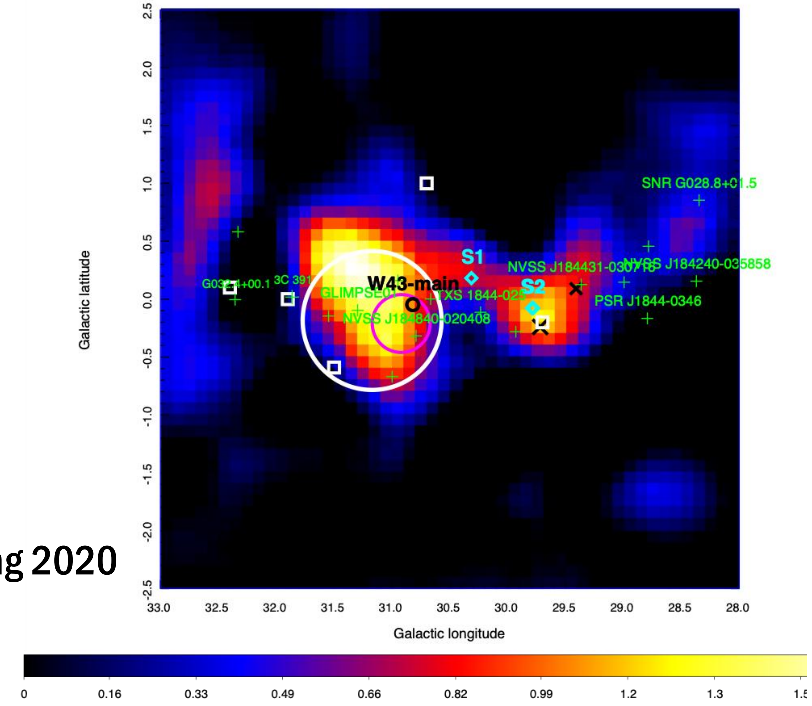

UHE gamma-ray emission from W43 is significantly detected, but the spectrum is very soft above 20-30 TeV

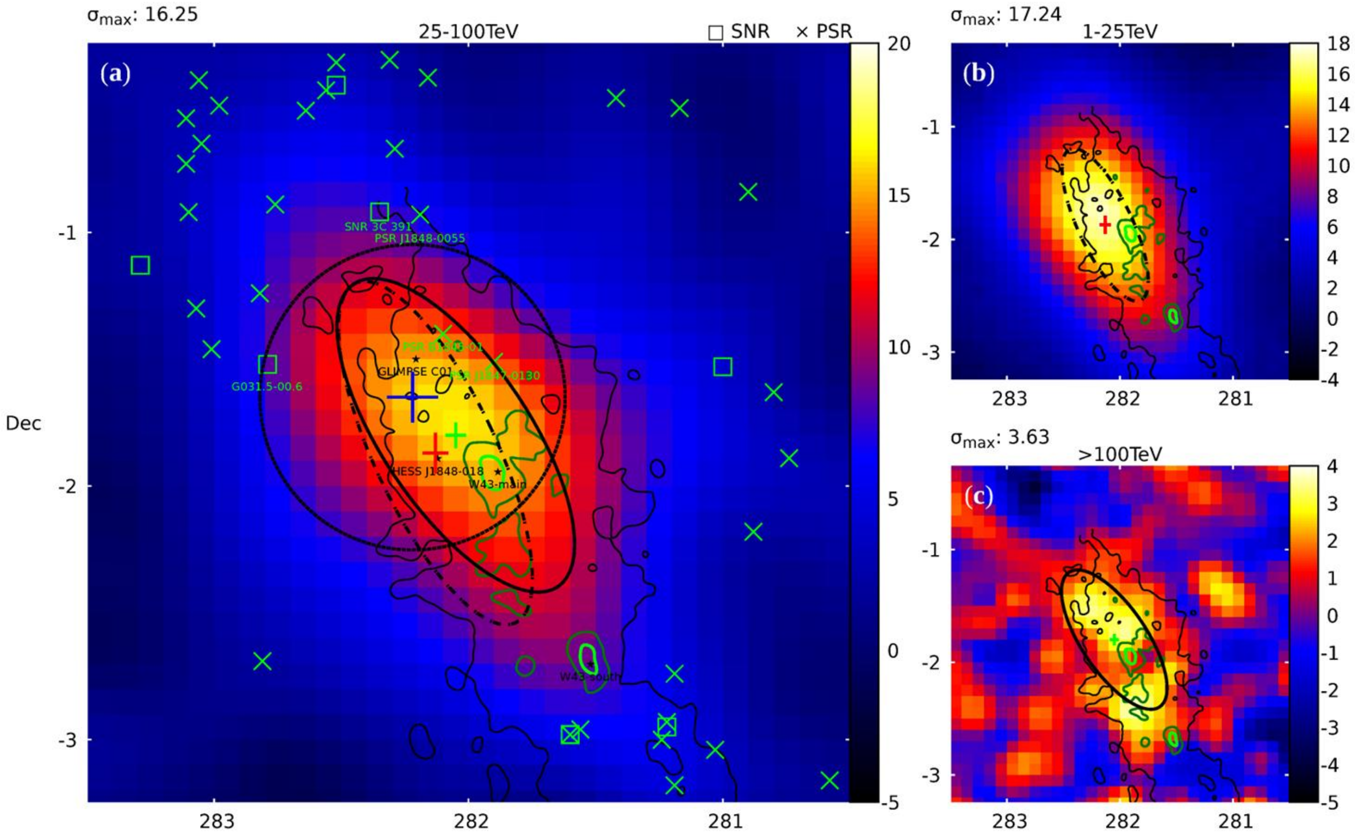

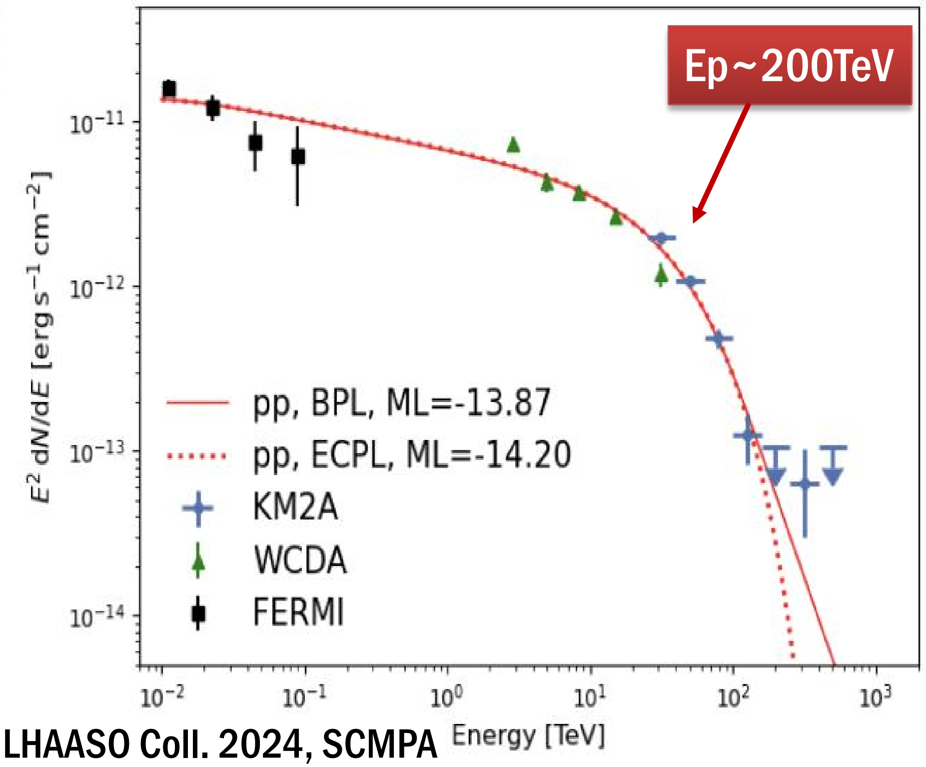

LHAASO Coll. 2024, SCMPA

W43 has higher SFR but less massive star than Cygnus OB2
What determines the particle acceleration capacity in young massive star cluster?

Summary

- LHAASO has detected a giant ultrahigh-energy gamma-ray bubble in Cygnus star-forming region, extending a radius of at least 6 deg
- Spectra and morphology of the bubble support the origin of UHE emission to be hadronic interactions of diffusing protons injected from the centra accelerator and surrounding gas
- Protons need be accelerated well beyond PeV in the central source. Cygnus OB2 is the best candidate of the super PeVatron, and the first-ever located source of CR at 10 PeV
- Observations of IACT with higher angular resolution toward the core region can reveal more physics. Accurate measurement of 3D gas distribution is crucial to understand the origin.

Thank you for your attention!

- Backup

Neutrinos

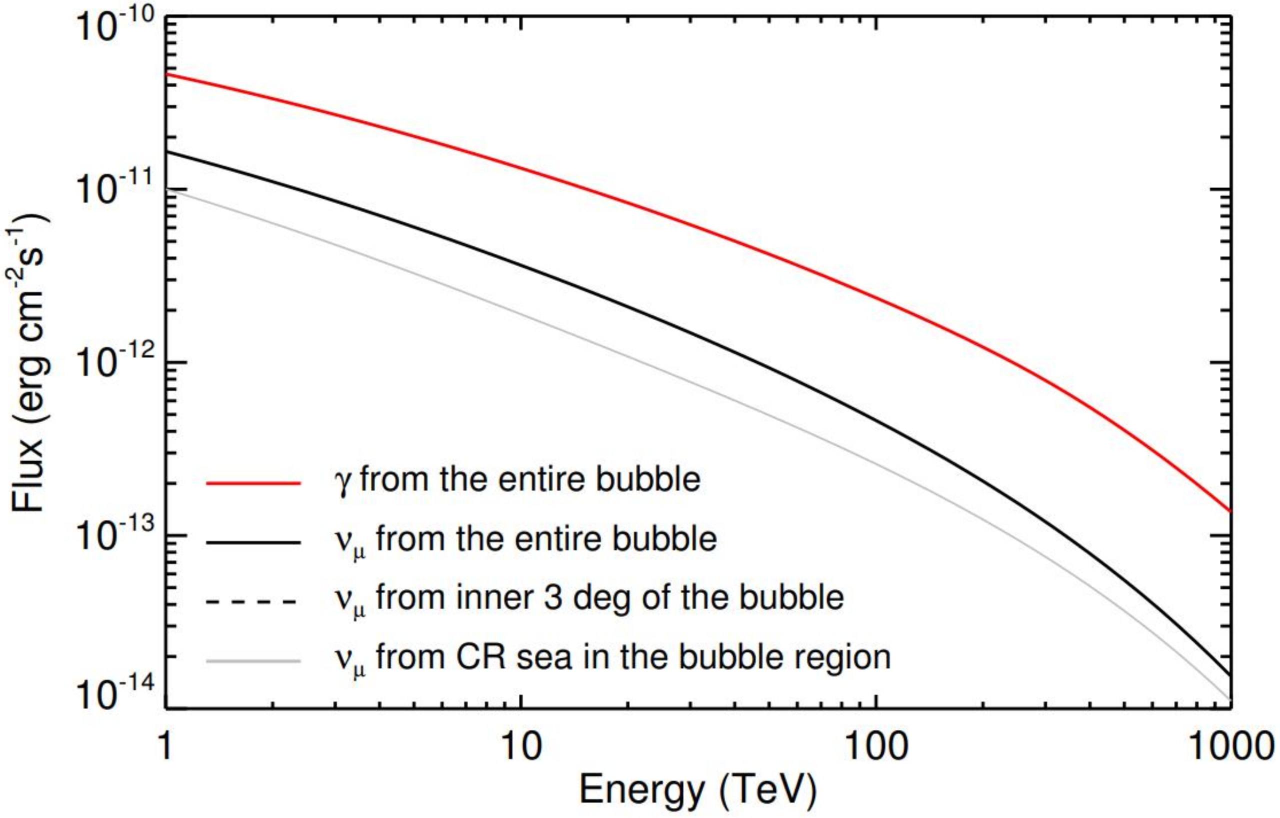

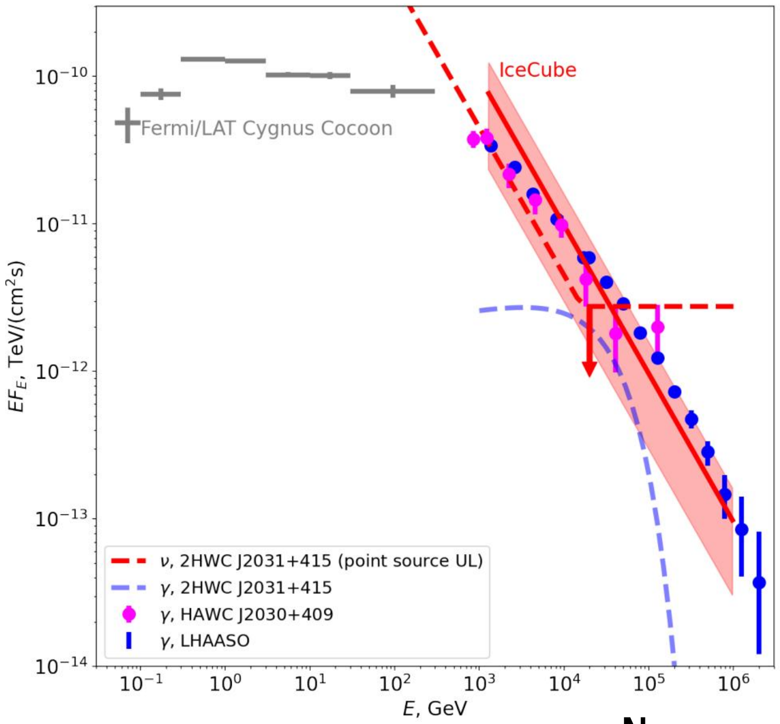

Neronov et al. 2023

29/7.7/0.36 (anti-)muon neutrino events above 1/10/100 TeV for 10-yr IceCube operation

Could other sources power the bubble?

Cygnus X-3

Unlikely.

Distance: 7.4

L ~ d^2 ~ 25 ↑

Much Less gas target at 7.4 kpc

L_{EDD} ~ 10^{39}erg/s

Required $L_p >> L_{EDD}$

PSR J2032+4127 / MT91 213

Unlikely.

L_{sd} ~ $1.7x10^{35}$ erg/s << required L_p

Binary emission – variable as measured by MAGIC & VERISTAS

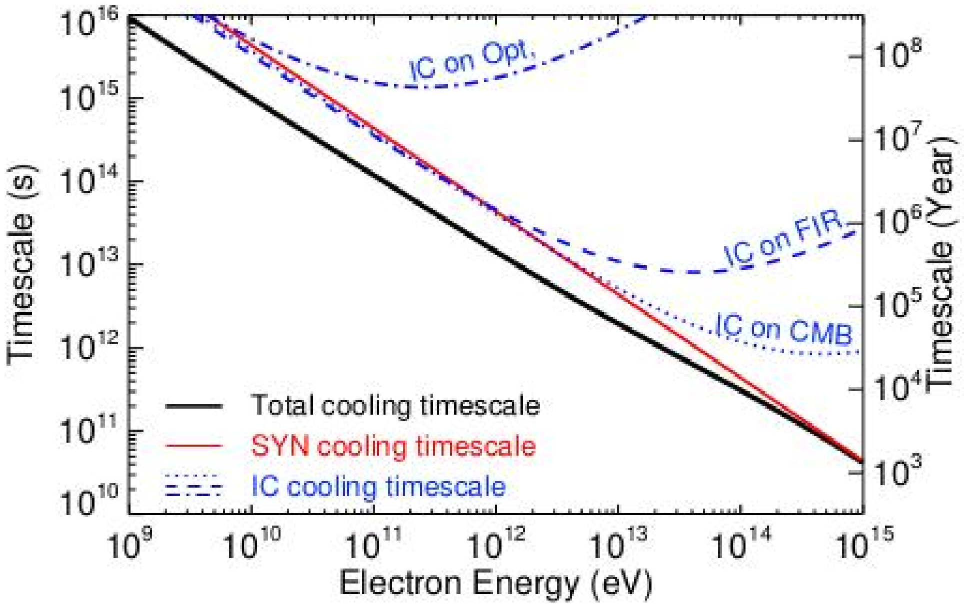

Influences on global CR transport in our Galaxy

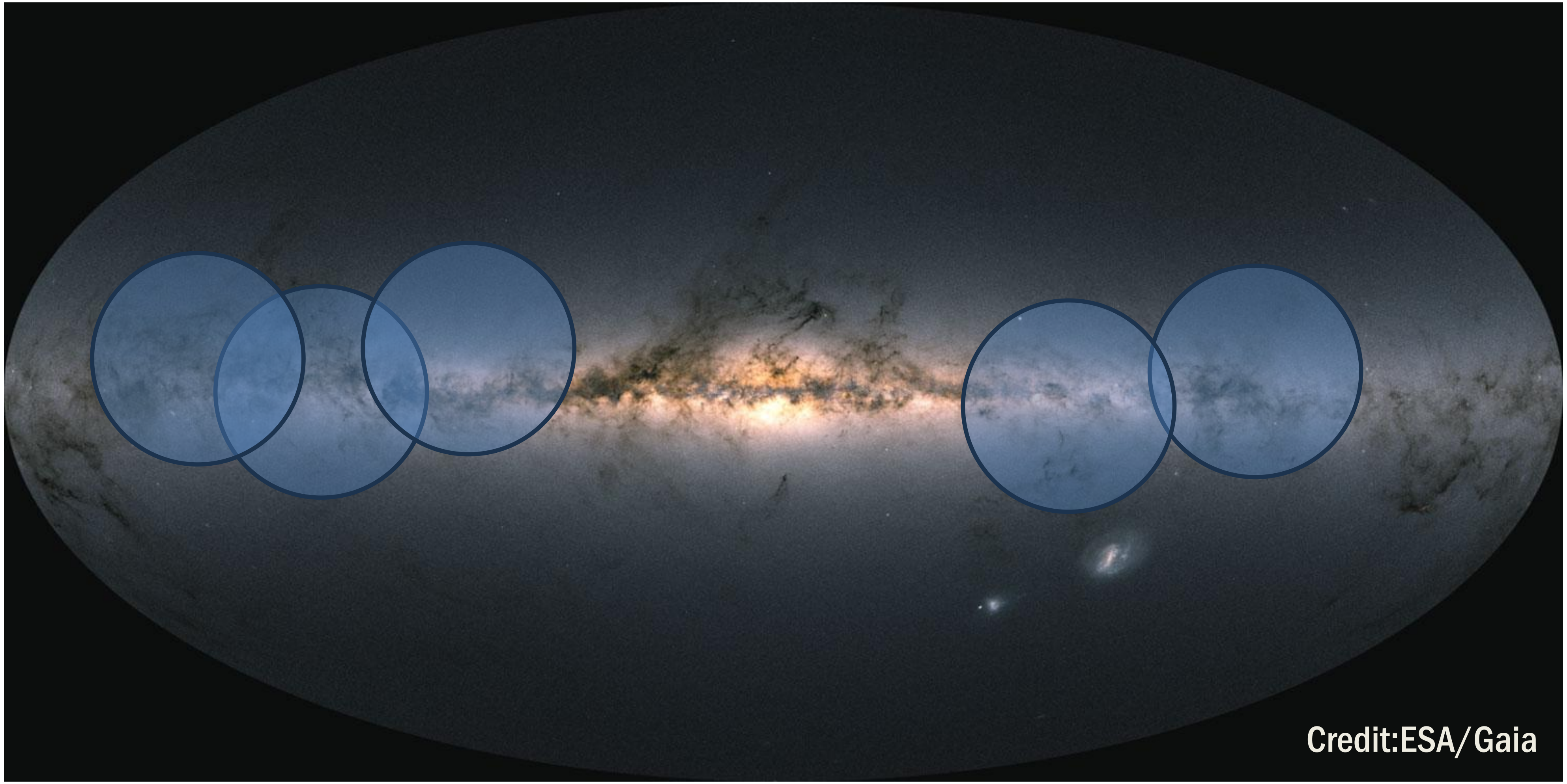

$D_{ISM} \sim 10(E/1GeV)^{1/2}$ from secondary-to-primary CR ratio

How common could such giant slow-diffusion bubble appear in Galaxy?

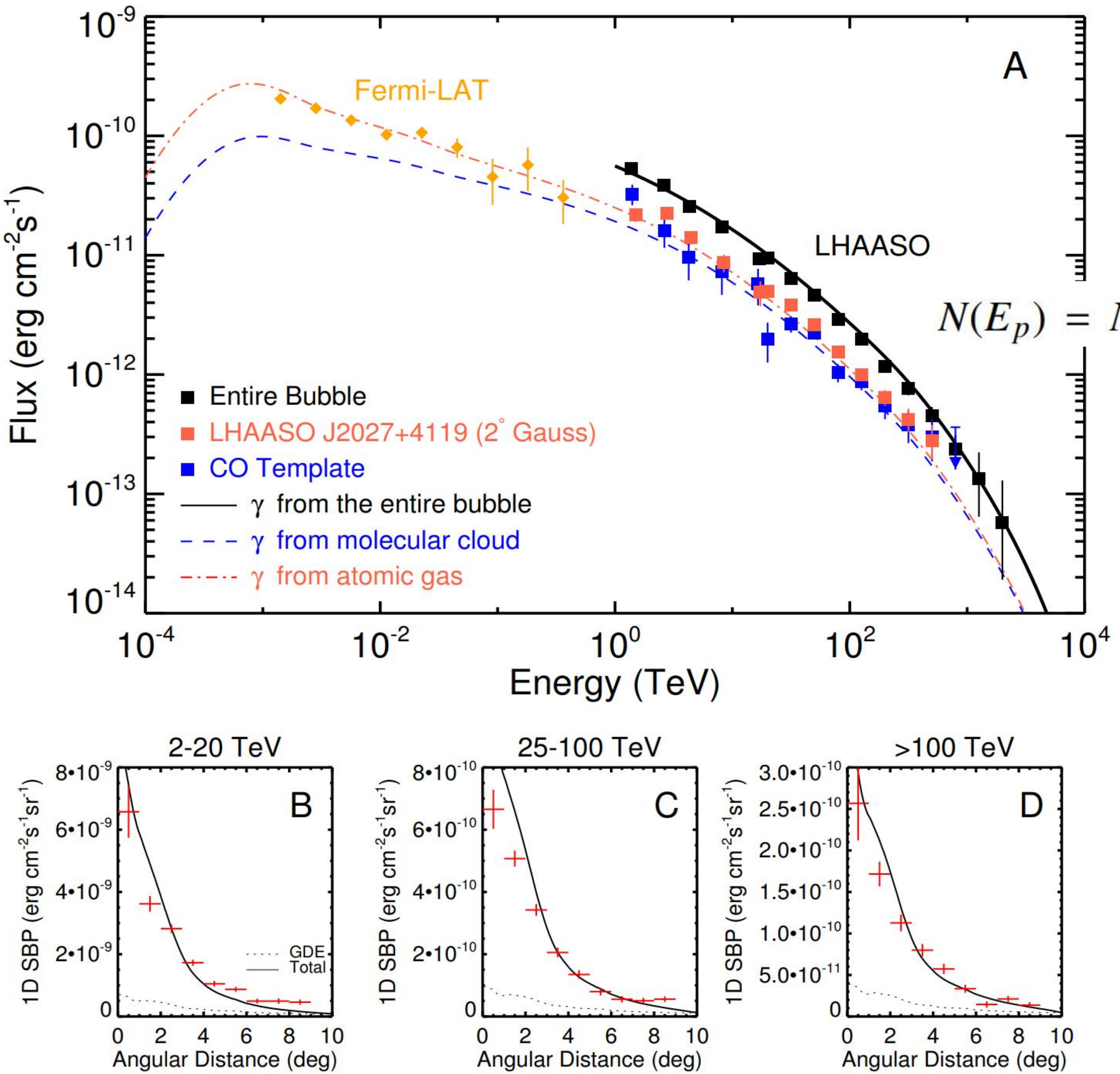

$$D(E_p) = 5\text{x}10^{26}\,(E_p/1\text{TeV})^{1/3}\ \text{cm}^2/\text{s}$$

$$N(E_p) = N_0 E_p^{-2.25}(1 + E_p/30\text{TeV})^{-0.5}\exp(-E_p/10\text{PeV}).$$

$$L_p \simeq 10^{37}\ \text{erg/s}$$